Initial evolution of high frequency enhanced ion line by X mode pump at EISCAT

Jun Wu[1], Jian Wu[1], Xuhui Shen[2], and Ingemar Haggstrom[3]

[1]National Key laboratory of electromagnetic environmentChina Research Institute of Radiowave Propagation(CRIRP)
[2]National Institute of Natural Hazards, Ministry of Emergency Management of China
[3]EISCAT Scientific Association

November 21, 2022

Abstract

During an experiment involving the alternating O / X mode pump, the observation demonstrated that the high frequency enhanced ion line (HFIL) and plasma line (HFPL) did not immediately appear after the pump onset, but were delayed by a few seconds. By examining the initial behaviors of the ion line, plasma line and electron temperature, it is found that (1) the HFIL and HFPL are delayed not only in the X pump mode but also in the O pump mode; (2) the HFIL can not be observed until the electron temperature is enhanced. The analysis reveals that (1) the leakage of the X mode to the O mode pump can not be ignored; (2) the electron temperature and the spatiotemporal uncertainty may play an important role in the lack of the Bragg condition; (3) nevertheless, the absence of parametric decay instability can not be ruled out due to the spatiotemporal uncertainty.

Title

Initial evolution of high frequency enhanced ion line by X mode pump at EISCAT

Authors and affiliations

(1) Jun Wu[1], (email: wujun1969@163.com)

(2) Jian Wu[1],

(3) Xuhui Shen[2],

(4) I. Haggstrom[3],

[1]National Key laboratory of electromagnetic environment, China research institute of radio wave propagation, Beijing 102206, China

[2] National Institute of Natural Hazards, Ministry of Emergency Management of China, Beijing, 100085, China

[3]EISCAT Scientific Association, Kiruna, Sweden

Key Points

(1) The delays of the high frequency enhanced ion line (HFIL) and plasma line (HFPL) can be induced by both the O / X mode pump.

(2) The HFIL can not be observed until the electron temperature is enhanced, namely, they are positively correlated.

(3)The spatiotemporal uncertainty at the critical altitude may also cause a lack of the Bragg condition and an under-dense condition.

Abstract

During an experiment involving the alternating O / X mode pump, the observation demonstrated that the high frequency enhanced ion line (HFIL) and plasma line (HFPL) did not immediately appear after the pump onset, but were delayed by a few seconds. By examining the initial behaviors of the ion line, plasma line and electron temperature, it is found that (1) the HFIL and HFPL are delayed not only in the X pump mode but also in the O pump mode; (2) the HFIL can not be observed until the electron temperature is enhanced. The analysis reveals that (1) the leakage of the X mode to the O mode pump can not be ignored; (2) the electron temperature and the spatiotemporal uncertainty may play an important role in the lack of the Bragg condition; (3) nevertheless, the absence of parametric decay instability can not be ruled out due to the spatiotemporal uncertainty.

Plain Language Summary

In the course of the ionospheric heating, the high frequency enhanced ion line (HFIL) and plasma line (HFPL) can not be induced by the X mode pump, and are immediately observed by the ultra high frequency incoherent scatter radar after the O mode pump onset. When the pump is operating in the alternating O / X mode near the critical frequency, however, an unexpected observation shows that the HFIL and HFPL can be induced by both the O mode and X mode pump, and do not immediately appear after the pump onset, but are delayed by a few seconds. With regard to the above observation, it is found that the HFIL does not appear until the electron temperature is enhanced. The analysis shows that the HFIL may be delayed due to the lack of the Bragg condition on the traveling path and the absence of the parametric decay instability at the critical altitude.

1. Introduction

The ionospheric modification theory and experiment have concluded that in the F region, the O mode pump can regularly induce numerous appreciable effects, but the X mode pump does not, due to the lower reflecting altitude of the X mode pump [*Robinson*, 1989; *Gurevich*, 2007, and references therein]. Recently, however, some effects similar to those induced by the O mode pump were induced by the X mode pump at the European Incoherent Scatter Scientific Association (EISCAT) [*Blagoveshchenskaya et al*., 2011, 2013, 2014, 2015, 2017a; *Borisova et al*., 2012]. In particular, it is distinctive that the high frequency enhanced ion line (HFIL) and plasma line (HFPL) did not immediately appear after the pump onset, but were delayed by 10 – 30 s [*Blagoveshchenskaya et al*., 2018, 2019, 2020].

Borisova et al. [2012] gave a hypothesis for the transformation of the X mode pump to the O mode pump in the anisotropic and nonuniform ionosphere and for the interaction between the X mode pump and the ionosphere. Thereafter, *Blagoveshchenskaya et al*. [2013, 2014, 2020] claimed that an adequate theory describing the interactions between the X mode pump and the ionosphere is absent, but they suggested that (1) the ohmic heating was not the only factor, (2) the enhanced electron density may be due to the ionization induced by electron acceleration, and (3) the HFIL and HFPL may involve mode conversion. In term of the HFIL and HFPL, *Wang et al*. [2016a, 2016b, 2017] proposed that a small parallel component of the X mode pump might satisfy the threshold and matching condition of the parametric decay instability (PDI) in an inhomogeneous plasma. Indeed, over the HFIL and HFPL induced by the X mode pump, there are some debates between *Blagoveshchenskaya et al*. [2017b] and *Wang et al*. [2016b, 2018].

In this letter, the initial behavior of the HFIL is examined by considering the electron temperature and the ionospheric condition at the critical altitude.

2. Experiment and measurements

The campaign involving the EISCAT heater and ultra high frequency incoherent scatter radar (UHF ISR) was conducted on 21 Feb. 2013, and was described in more detail by *Wang et al*. [2016b]. In brief, the heater and ISR were pointed at the geomagnetic field-aligned direction. With a heating cycle of 10 mins on and 5 mins off, the alternating O / X mode pump was operated at frequency $f_{\mathrm{HF}} = 7.1\ \mathrm{MHz}$ from 12:01 to 14:26 UT, and at $f_{\mathrm{HF}} = 5.423\ \mathrm{MHz}$ from 14:31 to 15:41 UT. It is important to note that f_{HF} was near the critical frequency f_0F_2. Unfortunately, however, f_0F_2 was not quiet and dropped as a whole during the experiment. The sharp drop or rise in f_0F_2 took place at 12:24, 12:40, 13:18, 14:12 and 14:54 UT, as shown in **Figure 1**. As a typical case, the measurement from 12:16 to 15:11 UT will be examined here.

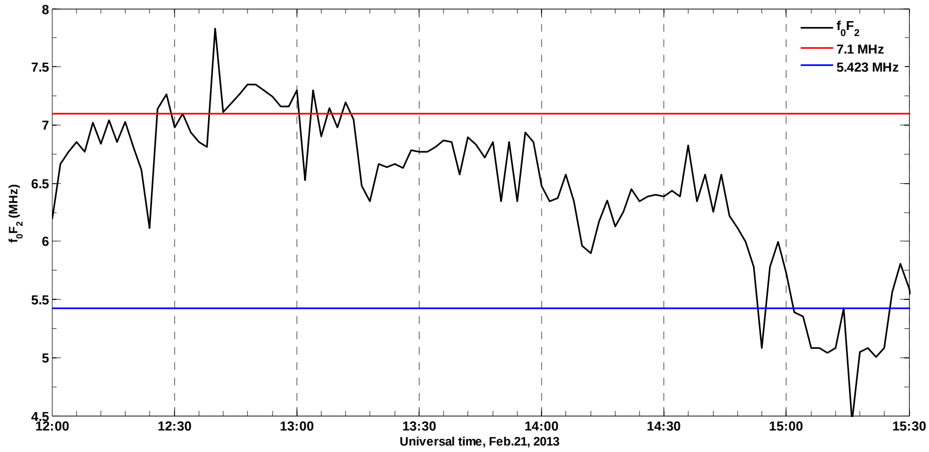

Figure 1. f_0F_2 recorded in ionosonde with a time resolution of 2 mins.

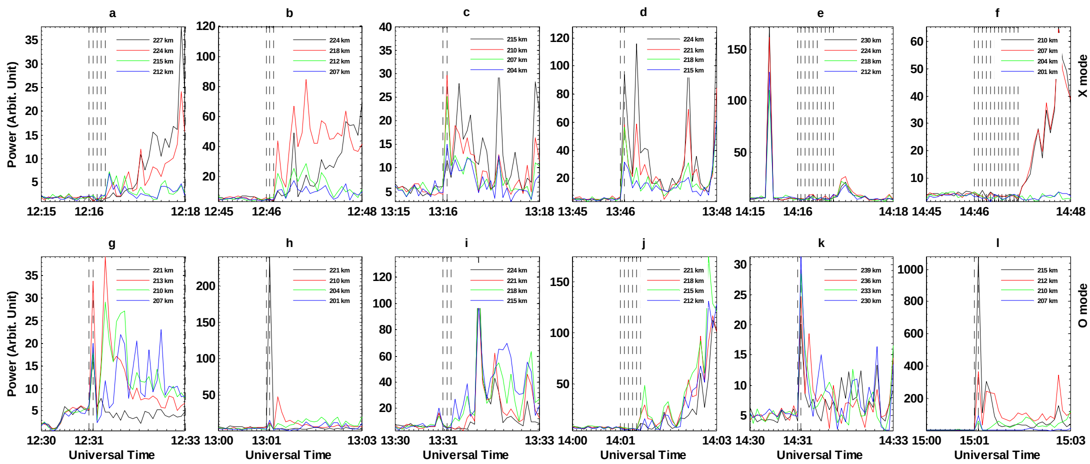

Figure 2. The initial evolution of ion line power at some altitudes, which are obtained through 5 s integration in the frequency range of -18 – 18 kHz by considering the PDI timescale of the order of millisecond [*Robinson*, 1989; *Gurevich*, 2007].

Figures 2 demonstrates the power of those ion lines in the last one minute before the pump onset and in the first two minutes after the pump onset. One can see that the HFIL is delayed by ~ 10 – ~ 55 s after the pump onset at 12:16, 12:46, 13:31, 14:01, 14:16 and 14:46 UT, whereas it immediately appears after the pump onset in the remaining heating cycles. Note that the delay of the HFIL has not shown the obvious dependence on the pump mode, although the HFIL is delayed more frequently in the X mode pump than in the O mode pump. In **Figure 3**, all of the HFPL are delayed for a longer time than the corresponding HFIL except those at 12:31, 13:01 14:31 and 15:01 UT.

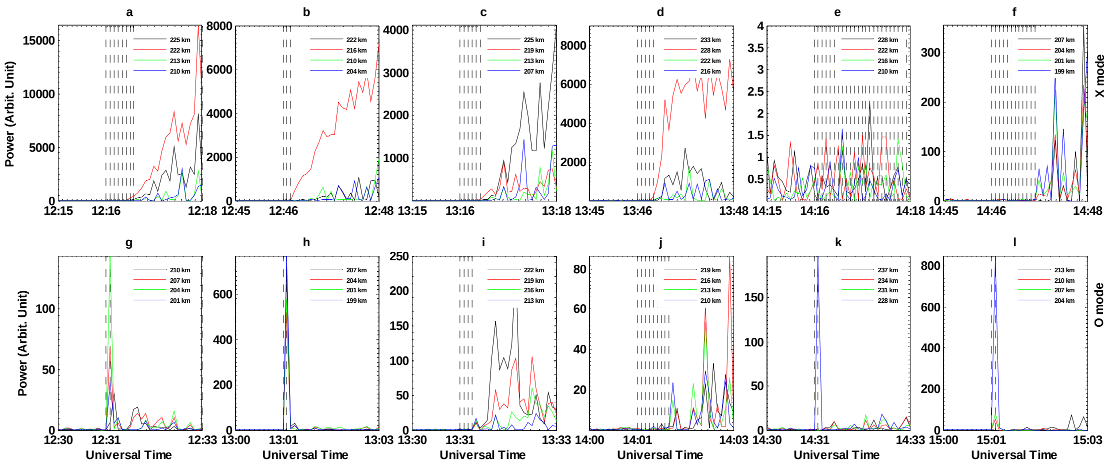

Figure 3. The same as **Figure 2**, but for plasma line, where (a) – (e) and (g) – (j) are integrated in the frequency range of 7 – 7.2 MHz, and (f), (k) and (i) are integrated in the frequency range of 5.323 – 5.523 MHz.

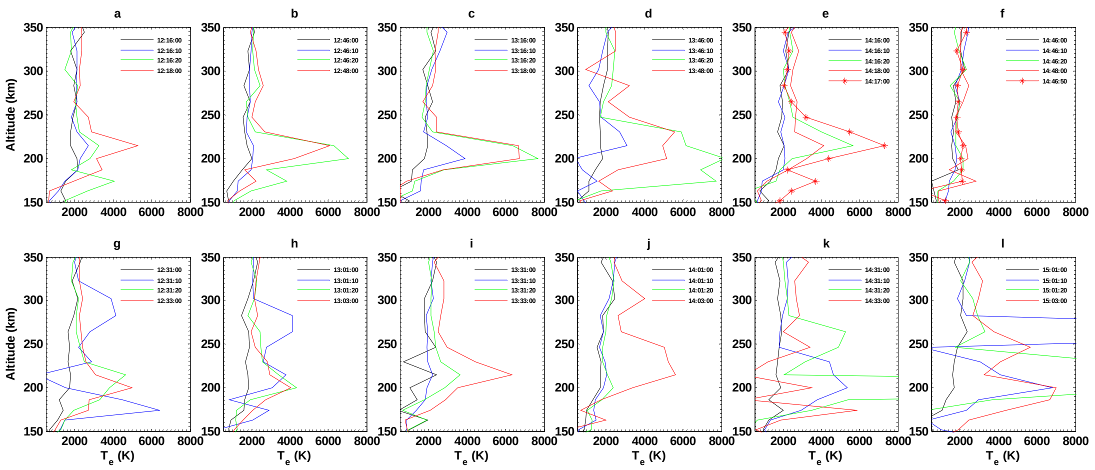

Figure 4. The initial evolution of T_e, which are obtained through 10 s integration by considering the electron temperature timescale of a few seconds [*Robinson*, 1989; *Gurevich*, 2007] and the HFIL delay of ~ 10 – ~ 55 s.

Figure 4 illustrates the electron temperature T_e in the altitude range of ~ 150 –

~ 350 km. It is evident that T_e is not significantly enhanced in 10 s after the pump onset at 12:16, 12:46, 13:31, 14:01, 14:16 and 14:46 UT, whereas it is enhanced in the remaining heating cycles. It is interesting to note that the initial evolution of T_e is temporally consistent with that of the ion line power shown in **Figure 2**, and has not shown the obvious dependence on the pump mode. Furthermore, T_e is enhanced in ~ 20 s after the pump onset in all of the cycles except that at 14:01 and 14:46 UT.

As an example, **Figure 5** illustrates some ion and plasma lines at 12:16:00, 12:16:20, 12:16:40, 12:17:00, 12:17:20, 12:17:40 and 12:18:00 UT at several altitudes. As might be expected, the ion and plasma lines are not enhanced at 12:16:00 UT. The HFILs of ~ 11.9 and ~ 13.1 kHz are observed in the time interval of 12:16:20 – 12:18:00 UT at altitude ~ 215 km. At altitude ~ 227 km, the HFILs of ~ 9.5 and ~ 11.9 kHz are respectively seen at 12:16:20 and 12:16:40 UT, and the HFIL of ~ 10.71 kHz appears in the time interval of 12:17:00 – 12:18:00 UT. Furthermore, no HFPL is obviously seen at altitude ~ 213 km., whereas at altitude ~ 225 km, the HFPL of ~ -7.091 MHz appears at 12;16:40 UT, and the HFPL of ~ -7.089 MHz appears at 12:17:00 – 12:18:00 UT.

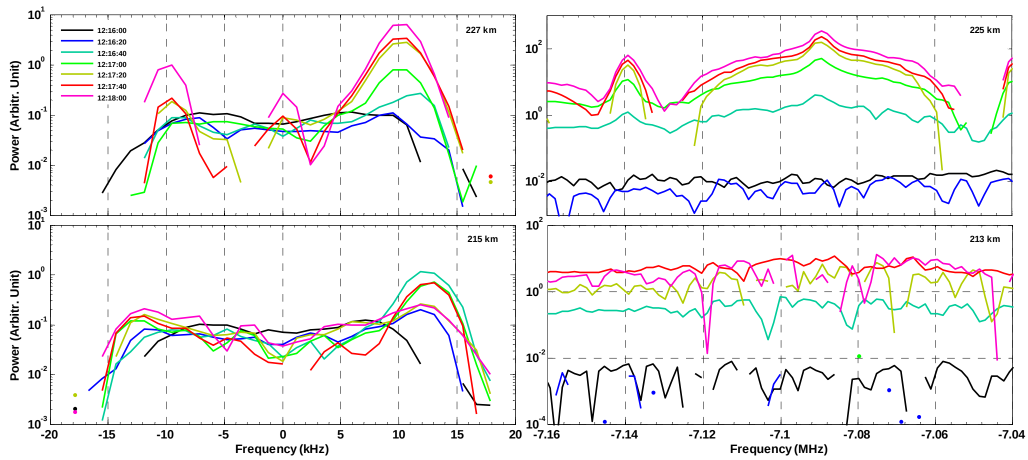

Figure 5. The ion and plasma lines in the time interval of 12:16:00 – 12:18:00 UT, which are obtained by integrating over a period of 20 s for the sake of smooth line.

3. Discussions

As demonstrated in **Figures 2** and **3**, not only the X mode pump but also the O mode pump induces the HFIL and HFPL as well as their delays. With regard to the ionospheric modification by the X mode pump, some studies have been carried out [*Borisova et al.*, 2012; *Blagoveshchenskaya et al.*, 2013, 2014, 2020; *Wang et al.*, 2016a, 2016b, 2017]. However, the leakage of the X mode pump to the O mode pump can not be ignored for the following reasons. (1) In reality, the EISCAT heater can not perfectively separate the O mode pump and the X mode pump [*Blagoveshchenskaya et al.*, 2014], and the leakage of the X mode pump to the O mode pump should be inevitable. (2) On the other hand, the O mode pump has a low threshold of ~ 17 – ~ 35 MW for the PDI in the typical ionosphere [*Robinson*, 1989; *Bryers et al.*, 2013], which may be satisfied by the leakage of the X mode pump to the O mode pump. (3) Despite the estimated leakage of ~ 2.3 – ~ 5 MW at the geomagnetic field-aligned direction [*Blagoveshchenskaya et al.*, 2014], one should be aware that the gain pattern of the EISCAT heater is modeled by assuming a perfectly reflecting ground [*Senior et al.*, 2011]. As a matter of fact, the ground at EISCAT in Tromsø is not a perfect reflector, but is composed of soil, dry sand, gravel, fine sediment and rock [*Senior et al.*, 2011]. (4) During the experiment, the ionosphere was quite active, whereas both of the O / X mode pump were operating at a constant frequency, that is, 7.1 MHz from 12:01 to 14:26 UT and 5.423 MHz from 14:31 to 15:41 UT. Thus, the spatiotemporal uncertainty at the critical altitude may make ionosphere over-dense, and then the PDI is excited at the critical altitude.

The lack of the Bragg condition for the enhanced acoustic wave should lead to the disappearance of the HFIL. In the case of backscattering, the ISR can only observe an ion acoustic wave satisfying the Bragg condition

$$k_{\mathrm{ia}} - 2k_{\mathrm{r}} = 0, \tag{1}$$

where k_{ia} and k_{r} denote the wave number of ion acoustic wave and the wave number of radar respectively. k_{ia} should follow the dispersion function

$$\omega_{\mathrm{ia}}^2 = \gamma \frac{K_{\mathrm{B}} T_{\mathrm{e}}}{m_{\mathrm{i}}} k_{\mathrm{ia}}^2, \tag{2}$$

where ω_{ia}, γ, K_{B} and m_{i} are the frequency of ion acoustic wave, the adiabatic index, Boltzmann constant and the effective ion mass respectively [*Baumjohann and Treumann*, 1997]. Having stated the above theoretical relation, the impact of T_e on the delay of the HFIL will be examined in the following.

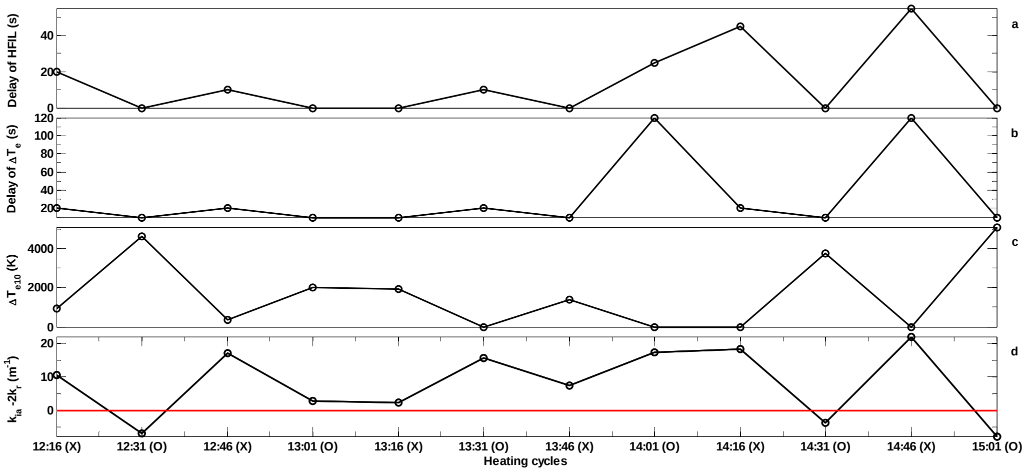

Figure 6. （a） The delay of the HFIL given by **Figure 2**, (b) the delay of the enhanced T_e given by **Figure 4**, (c) $\Delta T_{e10} = T_{e10} - T_{e0}$ at altitude ~ 200 km and (d) $k_{ia} - 2k_r$, where $k_{ia} = \sqrt{\dfrac{\omega_{ia}^2 m_i}{\gamma K_B T_{e10}}}$, $k_r = 19.5\ \mathrm{m}^{-1}$ for UHF radar at EISCAT, T_{e0} denotes the immediate electron temperature when the pump on, and T_{e10} denotes the electron temperature in 10 s after the pump onset, both of which are given by **Figure 4**. For the sake of simply computing, (1) $f_{ia} = 9.624\ \mathrm{kHz}$ is considered as the typical frequency of the HFIL during the experiment [*Wang et al*., 2016b, **Figure 3**]; (2) the effective ion mass is computed by $m_i = \dfrac{N_{O^+}}{N_e} m_{iO^+} + \left(1 - \dfrac{N_{O^+}}{N_e}\right) m_{iO_2^+}$, m_{iO^+} and $m_{iO_2^+}$ respectively denote oxygen atom mass and oxygen molecule mass, and the density ratio of O^+ to electron $\dfrac{N_{O^+}}{N_e}$ is obtained by International Reference Ionosphere 2007; (3) due to $m_{iO_2^+} \approx m_{iNO^+}$, O_2^+ and NO^+ are considered together; and (4) the profile of m_i is assumed to have not been modified by the pump due to the relatively massive ion.

By comparing **Figure 2** with **Figure 4**, one can find a spatiotemporally positive correlation between the delay of the HFIL and the delay of the enhanced T_e, as demonstrated in **Figures 6a** and **6b**. In the time interval of 12:16 – 13:46 UT, the HFIL delay of ~ 10 – ~ 20 s temporally corresponds to the ΔT_e delay of ~ 20 s, and the immediate HFIL temporally corresponds to the immediate ΔT_e. After 13:46 UT, the above behavior still holds, but the HFIL is delayed by ~ 25 – ~ 55 s and ΔT_e is delayed by ~ 25 – ~ 120 s. This may be due to the severe jitter of f_0F_2 in the time intervals of 14:00 – 14:20 UT and 14:46 – 15:00 UT as shown in **Figure 1**. Indeed, the measurement of f_0F_2 by ionosonde is rough, but the ionospheric trend should be available. Moreover, **Figures 6b** and **6c** demonstrate that at altitude ~ 200 km, there is a negative correlation between ΔT_{e10} and the delay of ΔT_e, which simply implies that when ΔT_e is delayed by ~ 20 s and more after the pump onset, T_e will not be enhanced in 10 s after the pump onset.

Next, k_{ia} can be obtained and be used to determine whether the Bragg condition is satisfied during the initial evolution, as shown in **Figure 6d**. At 12:16, 12:46, 13:31, 14:01, 14:16 and 14:46 UT, T_e is not significantly enhanced in 10 s after the pump onset, then $k_{ia} - 2k_r$ is successively ~ 10.6, ~ 17, ~ 15.7, ~ 17.4, ~ 18.3 and ~ 22 m^{-1}, which are remarkably deviate from zero. Namely, k_{ia} does not significantly satisfy $k_{ia} = 2k_r$ and the HFIL should not be observed by the ISR. Otherwise, at 12:31, 13:01, 13:16, 13:46, 14:31 and 15:01 UT, T_e is significantly enhanced up to ~ 2500 – ~ 5000 K in 10 s after the pump onset, then $k_{ia} - 2k_r$ is successively ~ -6.8, ~ 2.8, ~ 2.4, ~ 7.4, ~ -3.8 and ~ -7.7 m^{-1}, which are slightly deviates from zero. In other words, k_{ia} does approximately satisfy the Bragg condition and the ISR can observe those enhanced ion acoustic wave. Indeed, those enhanced ion acoustic waves within a small range of k_{ia} may contribute to the HFIL. In addition, when $\Delta T_{e10} \approx\sim$ 2000 K at 13:01, 13:16 and 13:46 UT, $k_{\mathrm{ia}} - 2k_{\mathrm{r}}$ positively approaches to zero, whereas $k_{\mathrm{ia}} - 2k_{\mathrm{r}}$ negatively approaches to zero when $\Delta T_{\mathrm{e}10} >\sim 3800\ \mathrm{K}$ at 12:31, 14:31 and 15:01 UT. This implies that in present case, when $\Delta T_{\mathrm{e}10} \approx 2800\ \mathrm{K}$, $k_{\mathrm{ia}} - 2k_{\mathrm{r}} \approx 0$, namely, the Bragg condition can exactly be satisfied. This seems imply that the interaction between the pump and ionosphere may have taken place during the initial evolution, but the HFIL is not observed due to the lack of $k_{\mathrm{ia}} \approx 2k_{\mathrm{r}}$ at 12:16, 12:46, 13:31, 14:01, 14:16 and 14:46 UT.

Besides the impact of T_{e} on the traveling path, the HFIL may not be observed due to spatiotemporal uncertainty of the ionosphere at the critical altitude. In those over-dense conditions at 12:16 and 14:46 UT, the sharp decrease of ~ 1 MHz in the critical frequency implies that the ionosphere should be intensely active and the ion profile may be significantly modified, thus the HFIL may not be observed due to the lack of the Bragg condition. At 15:01 UT, however, the critical frequency sharply decrease from ~ 6 MHz to ~ 5 MHz, but the HFIL is not delayed. Moreover, one can find by comparing **Figures 2** and **3** that the HFPL is delayed by a longer time than the corresponding HFIL, for instance, the HFPL by ~ 20s and the HFPL by ~ 35s at 12:16 UT, which is not consistent with those regular experimental results [*Robinson*, 1989]. The fact is that the enhanced ion acoustic and Langmuir waves are simultaneously induced by the PDI on the timescale of the order of milliseconds [*Robinson*, 1989; *Gurevich*, 2007]. This implies that the Bragg conditions of the enhanced ion acoustic and Langmuir waves are not simultaneously satisfied on their traveling paths.

Nevertheless, it can not be ruled out that the PDI has not been excited in the initial evolution. As a case, those ion and plasma lines in the time interval of 12:16:00 – 12:18:00 UT are examined, as illustrated in **Figure 5**. As expected, those ion and plasma lines are not enhanced at 12:16:00 UT. In the time interval of 12:16:20 – 12:18:00 UT, the HFIL of ~ 11.9 kHz appears at altitude ~ 212 km, whereas no obvious HFPL is found at altitude ~ 213 km. A possible explanation is that during this period, the HFIL may not have been induced by the pump, but the natural ion acoustic wave at 11.9 kHz may satisfy the Bragg condition due to the enhanced T_{e} on the traveling path. Here the natural ion acoustic wave denotes those not enhanced by the pump. Indeed, the natural ion acoustic wave covers a wide frequency spectrum due to the wide spectrum of ion mass distribution in ionosphere. Considering $f_{\mathrm{ia}} = 11.9\ \mathrm{kHz}$, $T_{\mathrm{e}} \approx 3200\ \mathrm{K}$ and $m_{\mathrm{i}} = 3.72\times10^{-26}\ \mathrm{kg}$ computed as in **Figure 6**, thus $k_{\mathrm{ia}} \approx 39.6\ \mathrm{m}^{-1}$. In other word, when $T_{\mathrm{e}} \approx 3200\ \mathrm{K}$, the natural ion line of 11.9 kHz should be observed by the ISR. Further, in the time interval of 12:17:00 – 12:18:00 UT, it is evident that the HFIL of 10.71 kHz is observed at altitude ~ 227 km, which is an exact match for the HFPL of 7.089 MHz observed at altitude ~ 225 km, as indicated by the matching frequency $f_{\mathrm{HF}} = f_{\mathrm{L}} + f_{\mathrm{ia}}$, where f_{L} is the HFPL frequency. The above analysis implies that due to the enhanced T_{e} on the traveling path, the natural ion acoustic wave may approximately satisfy the Bragg condition and may contribute to the enhanced ion line power in the time interval of 12:16:20 – 12:17:00 UT, whereas the PDI has not been excited until 12:17:00 UT. This may be the so-called "pre-condition" suggested by *Blagoveshchenskaya et al*. [2020].

Moreover, the spatiotemporal uncertainty at the critical altitude may make the ionosphere under-dense and lead to the absence of the PDI. One can see in **Figure 2** that the HFIL is delayed at 13:31, 14:01 and 14:16 UT, when the ionosphere is in the under-dense condition of ~ 6.5 MHz and is basically quiet as in **Figure 1**. However, it is unexpected that the HFIL is delayed by 10 s in the over-dense condition of ~ 7.25 MHz at 12:46 UT, whereas it is not delayed in the under-dense condition of ~ 6.5 MHz at 13:16 and 13:46 UT. Nevertheless, the under-dense condition should be a important factor in the study of delay of HFIL in the initial evolution. Indeed, the O / X mode pump were operating at $f_{\mathrm{HF}} \approx f_0\mathrm{F}_2$, whereas $f_0\mathrm{F}_2$ is not quiet in the present ionosphere.

4. Summary and conclusions

The experiment involving the EISCAT heater and UHF ISR was carried out at

EISCAT. The observation demonstrates that in some heating cycles, the HFIL and HFPL did not immediately appear after the pump onset, but were delayed by a few seconds.

The fact is that the O / X mode pump can both induce the delays of the HFIL and HFPL, and the delays of the HFIL and HFPL appears more frequently in the X mode pump than in the O mode pump. Considering the inevitable leakage of the EISCAT heater, the gain pattern model error, the low threshold of PDI and the spatiotemporal uncertainty at the critical altitude, the leakage of the X mode pump to the O mode pump should not be ignored.

In the initial evolution, there is a spatiotemporally positive correlation between the delay of HFIL and the delay of enhanced T_e, implying that the delay of the enhanced T_e may cause the delay of the HFIL. That is, the PDI may have been excited immediately after the pump onset, but the Bragg condition may not be satisfied so that the HFIL should not be observed by the ISR until T_e is enhanced up to ~ 2500 – ~ 5000 K on the traveling path. Besides, in the initial evolution, the spatiotemporal uncertainty at the critical altitude may result in the lack of the Bragg condition, and then the HFIL is delayed.

It can not be ruled out that the PDI has not been excited in the initial evolution. A case study shows that due to the enhanced T_e, the natural ion line contributes to the power of HFIL in the initial evolution. Similarly, the spatiotemporal uncertainty at the critical altitude may make a significant impact on the interaction between the O / X mode pump and the ionosphere, and the under-dense heating can not be ignored. Indeed, a quiet ionosphere should be pursued and the further investigation is expected.

Acknowledgments

EISCAT is an international scientific association supported by China, Finland, Japan, Norway, Sweden and the UK. Authors thank Russian colleagues for their significant efforts in performing experiment, and Dr. Michael. T. Rietveld for the productive discussion on the gain pattern of EISCAT heater. The data can be obtained

at https://portal.eiscat.se/schedule/

References

1. Banmjohann Wolfgang & Rudolf A. Treumann (1997), Basic space plasma physics. *Imperial College press*.

2. Blagoveshchenskaya, N. F. , Borisova, T. D. , Kalishin, A. S., Yeoman, T. K., & Häggström, I. (2017a), First observations of electron gyro-harmonic effects under x-mode hf pumping the high latitude ionospheric f-region. *J. Atmos. Sol. Terr. Phys*., 155, 36-49.

3. Blagoveshchenskaya, N. F., Borisova, T. D., & Yeoman, T. K. (2017b), Comment on“Parametric instability induced by X-mode wave heating at EISCAT” by Wang et al. (2016). *J. Geophys. Res.* Space Physics, 122, 12570 – 12585. https://doi.org/10.1002/2017JA023880

4. Blagoveshchenskaya, N. F., Borisova, T. D., Kalishin, A. S., Kayatkin, V. N., Yeoman, T.K. & Haggstrom, I. (2018), Comparison of the Effects Induced by the Ordinary (O-Mode) and Extraordinary (X-Mode) Polarized Powerful HF Radio Waves in the High-Latitude Ionospheric F Region. *Cosmic Research*, 56, 1, 16.

5. Blagoveshchenskaya, N. F., Borisova, T. D., Kalishin, A. S., Yeoman, T. K., & Häggström, I. (2020), Distinctive features of Langmuir and ion ‐ acoustic turbulences induced by O – and X – mode HF pumping at EISCAT. *J. Geophys. Res.* Space Physics, 125, e2020JA028203. doi :10.1029/2020JA028203.

6. Blagoveshchenskaya, N. F., Borisova, T. D., Kosch, M., Sergienko, T., Brändström, U., Yeoman, T. K., & Häggström, I. (2014), Optical and ionospheric phenomena at EISCAT under continuous X – mode HF pumping. *J. Geophys. Res*. Space Physics, 119, 10483–10498. doi:10.1002/ 2014JA020658.

7. Blagoveshchenskaya, N. F., Borisova, T. D., Yeoman, T. K., Häggström, I., & Kalishin, A. S. (2015), Modification of the high latitude ionosphere F region by X – mode powerful HF radio waves: Experimental results from multi-instrument diagnostics. *J. Atmos. Sol. Terr. Phys*., 135, 50 – 63. doi:10.1016/j.jastp.2015.10.009.

8. Blagoveshchenskaya, N. F., Borisova, T. D., Yeoman, T. K., Rietveld, M. T., Ivanova, I. M. & Baddeley, L. J. (2011), Artificial field-aligned irregularities in the high-latitude F region of the ionosphere induced by an X-mode HF heater wave. *Geophys. Res. Lett.*, 38, L08802. doi:10.1029/ 2011GL046724.

9. Blagoveshchenskaya, N. F., Borisova, T. D., Yeoman, T. K., Rietveld, M. T., Häggström, I. & Ivanova, I. M. (2013), Plasma modifications induced by an X-mode HF heater wave in the high latitude F region of the ionosphere. *J. Atmos. Sol. Terr. Phys.*, 105-106, 231–244. doi:10.1016/j.jastp.2012.10.001.

10. Blagoveshchenskaya,N. F., Borisova,T. D., Kalishin, A. S., Yeoman, T. K. & Haggstrom, I. (2019), Artificial plasma turbulence in the high latitude ionosphere F region induced by extraordinary polarized HF pump wave at EISCAT. 19th International EISCAT Symposium, 19th - 23rd August 2019, Oulu, Finland.

11. Borisova, T. D., Blagoveshchenskaya, N. F., Kalishin, A. S., Oksavik, K., Baddelley, L. & Yeoman, T. K. (2012), Effects of modification of the polar ionosphere with high-power short-wave extraordinary-mode HF waves produced by the spear

heating facility. *Radiophysics and Quantum Electronics*, 55, 1–2.

12. Bryers C. J., M. J. Kosch, A. Senior, M. T. Rietveld & T. K. Yeoman (2013), The thresholds of ionospheric plasma instabilities pumped by high-frequency radio waves at EISCAT, *J. Geophys. Res.*: Space Physics, 118, 7472, doi:10.1002/2013JA019429.
13. Gurevich, A. V. (2007), Nonlinear effects in the ionosphere. *Physics Uspekhi*, 50(11), 1091.
14. Robinson, T. R. (1989), The heating of the high latitude ionosphere by high power radio waves. *Physics Reports*, 179, 2 & 3, 79.
15. Senior, A., Rietveld, M. T., Honary, F., Singer, W. & Kosch, M. J. (2011), Measurements and modeling of cosmic noise absorption changes due to radio heating of the D region ionosphere. *J. Geophys. Res.*, 116, A04310. doi:10.1029/2010JA016189.
16. Wang, X. & Zhou, C. (2017), Aspect dependence of Langmuir parametric instability excitation observed by EISCAT. *Geophys. Res. Lett.*, 44. doi:10.1002/2017GL074743.
17. Wang, X., Zhou, C., Liu, M., Honary, F., Ni, B. & Zhao, Z. (2016b), Parametric instability induced by X-mode wave heating at EISCAT. *J. Geophys. Res*. Space Physics, 121, 10, 536–10548. doi:10.1002/2016JA023070.
18. Wang, X., Cannon, P., Zhou, C., Honary, F., Ni, B. & Zhao, Z. (2016a), A theoretical investigation on the parametric instability excited by X – mode polarized electromagnetic wave at Tromsø. *J. Geophys. Res*. Space Physics, 121, 3578 –3591. doi:10.1002/2016JA022411.
19. Wang, X., Zhou, C. & Honary, F. (2018), Reply to comment on the article “Parametric Instability Induced by X-Mode Wave Heating at EISCAT” by Wang et al. (2016). *J. Geophys. Res*. Space Physics, 123, 8051 – 8061. https://doi.org/10.1029/2018JA025808.